their $6S_4$. Notice, however, that we have not followed this reference in the character tables for $\bar{S}_4$, $\bar{C}_3$, and $\bar{C}_{1h}$. In fact, the character table for $\bar{S}_4$ is incorrect in this reference.

[11]D. F. Johnston, S. Marlow, and W. A. Runciman, J. Phys. C 1, 1455 (1968).

[12]S. Rodriguez, P. Fisher, and F. Barra, Phys. Rev. B 5, 2219 (1972).

[13]Silicon: G. Feher, J. C. Hensel, and E. A. Gere, Phys. Rev. Letters 5, 309 (1960); germanium: R. L. Jones and P. Fisher, Phys. Rev. B 2, 2016 (1970).

[14]J. M. Luttinger, Phys. Rev. 102, 1030 (1956).

[15]G. F. Koster, Phys. Rev. 109, 227 (1958).

[16]H. P. Soepangkat, P. Fisher, and S. Rodriguez, Phys. Letters 39A, 379 (1972).

[17]R. L. Jones and P. Fisher, J. Phys. Chem. Solids 26, 1125 (1965).

[18]K. S. Mendelson and H. M. James, J. Phys. Chem. Solids 25, 729 (1964).

[19]E. Merzbacher, *Quantum Mechanics*, 2nd ed. (Wiley, New York, 1970), p. 316.

PHYSICAL REVIEW B VOLUME 6, NUMBER 10 15 NOVEMBER 1972

Linewidths and Two-Electron Processes in Spin-Flip Raman Scattering from CdS and ZnSe

J. F. Scott,* T. C. Damen, and P. A. Fleury
Bell Telephone Laboratories, Holmdel, and Murray Hill, New Jersey 07974

(Received 9 May 1972)

We present inelastic-light-scattering data and analyses for spin-flip scattering from conduction electrons in CdS and ZnSe. Cross sections, linewidths, and line shapes are studied as functions of magnetic field, temperature, scattering angle, and donor concentration. Both free-conduction-electron spin-flip processes and spin-flip processes involving conduction electrons bound to shallow donors are observed. These processes exhibit different selection rules and temperature dependences; the free-electron spin-flip processes exhibit only α_{ij} scattering in which $i \neq j$ and i or $j \parallel \vec{H}$ as expected, while the bound-electron spin-flip processes also exhibit strong α_{xx} and α_{yy} scattering (z is the [0001] optic axis), in agreement with the selection rules calculated for shallow donors at C_{3v} Cd sites by Thomas and Hopfield. For right-angle scattering, the free-electron linewidth increases from 0.05 cm^{-1} (half-width at half-height) at 2 °K to about 4 cm^{-1} at ~150 °K in both ZnSe and CdS. This broadening is not due to a decrease in spin lifetime, but rather to a spin diffusion, as directly confirmed by the angular dependence of the spin-flip linewidth. The linewidth is observed to vary as q^2, where q is the momentum transfer in the light-scattering process. Bound-electron scattering exhibits a linewidth which is independent of scattering angle and nearly independent of temperature over the 2–150 °K range. The spin-diffusion model is thus not applicable to bound-electron scattering. The double spin-flip process observed involves two interacting electrons with an apparent attractive energy of 0.25 ± 0.05 cm^{-1}. Selection rules, relative cross sections, field dependence, and binding energy of the double spin-flip transition are discussed. At sufficiently high input powers (≥ 3 MW/cm^2) the CdS single spin-flip scattering becomes stimulated, resulting in a tunable, visible, spin-flip laser.

I. INTRODUCTION

In an earlier paper[1] we reported spin-flip scattering from free conduction electrons in the wide-gap semiconductors CdS and ZnSe. Reference 1 emphasized the determination of selection rules, gyromagnetic ratios (g values), and absolute scattering cross section and indicated the existence of anomalous linewidths. In the present work[2] we have systematically studied the spin-flip line shapes, the dependence of linewidth upon temperature, magnetic field, and scattering angle, and change in selection rules as the sample temperature is reduced below the exciton binding energy. We have examined scattering cross sections as functions of several parameters (temperature, field, laser power, laser frequency, donor concentration); and finally, we have studied a new two-electron scattering process involving simultaneous spin-flip scattering of two electrons bound to nearby donors. The latter process is highly resonant, involves a total spin change of $\Delta S = \pm 2$, and exhibits a spin-spin interaction energy of 0.03–0.04 meV (0.2–0.3 cm^{-1}).

In Sec. II we present line-shape and linewidth measurements as functions of temperature, field, and scattering angle. In Sec. III we present temperature and field dependences of cross sections and briefly mention the observation of stimulated spin-flip scattering in CdS. In Sec. IV the selection rules at different temperatures are discussed. Section V is concerned with the double spin-flip process, including its selection rules, resonant cross sections, and dependence upon donor concentrations.

The basic theory of spin-flip scattering is at

this time well known. Experiments on free-electron spin-flip processes have been reported on InSb,[3] InAs,[4] and PbTe,[5] in addition to CdS and ZnSe.[1] Bound-electron spin-flip scattering in CdS was studied in some detail by Thomas and Hopfield,[6] who concluded that both electrons and holes bound to shallow impurities yield very large cross sections. Electrons (or holes) and photons in the crystals interact according to the Hamiltonian

$$H=(1/2M)\sum_i[\vec{p}_i-(e/c)\vec{A}]^2 \quad , \tag{1}$$

where $\vec{p}_i$ is the momentum of the ith electron and $\vec{A}$ is the vector potential of the electromagnetic (photon) field. Inelastic spin-flip scattering in a semiconductor requires only two things, as diagrammed in Fig. 1: a finite spin-orbit coupling, so that the valence band shown is neither pure spin up nor pure spin down; and an external magnetic field, which splits the electron-spin levels in the conduction band by $\hbar\Delta\omega=\mu_B gH$. The spin-flip scattering arises from the interband $\vec{p}\cdot\vec{A}$ matrix elements between the conduction band and the spin-orbit-split valence band. Other mechanisms for spin-flip scattering have been proposed[7] but have not been observed to date.

The prospect of observing spin-flip scattering from mobile carriers in the visible portion of the spectrum was first suggested by the electron-scattering experiments on CdS in zero field, where both collective-plasmon and single-particle electron scattering were observed.[8] Such $H=0$ scattering for CdS with $n\cong 4\times10^{18}$ cm^{-3} is shown in Fig. 2 for α_{xz} scattering (z is the optic axis). For single-particle scattering from a degenerate electron gas, the spectrum in absence of collisions at zero temperature should increase linearly with frequency shift, peak at about $0.75qV_F$, and terminate abruptly at qV_F.[9] V_F is the Fermi velocity, q is the wave-vector transfer. The combined effects of nonzero temperature and particle collisions distort the observed spectrum in Fig. 2 from this simple shape. Figure 3 shows a similar spectrum for nondegenerate CdS with $n\cong1\times10^{16}$ cm^{-3}. The observed spectral distribution function in Fig. 3 can be reasonably described by a simple Gaussian form

$$I(\omega)=I_0e^{-\omega^2/A(T)} \quad . \tag{2}$$

Ordinarily for single-particle Doppler-shifted scattering in the absence of collisions, $A(T)$ is a product of the squares of the momentum transfer q and the thermal velocity $v_{\rm th}$ for particles obeying a Maxwell–Boltzmann velocity distribution.[10] However, the $v_{\rm th}$ required to fit the data of Fig. 3 corresponds to too high a temperature ($T=133$ °K). The excess width is probably due to collision effects, since the electron collision time for this sample is $\sim10^{-13}$–10^{-14} sec. As the temperature increases, both the intensity and width of the single-electron scattering increase. These spectra are observed as background "skirts" or "plateaus" on all our spin-flip data. Moreover, they appear for some polarizations where free-electron spin-flip scattering is forbidden. For example, at 130 °K and 80 kG, spin-flip scattering is observed in $n=10^{17}$ cm^{-3} CdS only for α_{xy} and α_{zy} with the field along y, but very strong single-electron (no-flip) scattering is manifest for α_{xz}. The fact that the single-electron scattering is observed for off-diagonal polarizability-tensor components indicates that it arises from spin-density fluctuations rather than charge-density fluctuations, which are subject to efficient screening in high-carrier-concentration semiconductors.[9,10]

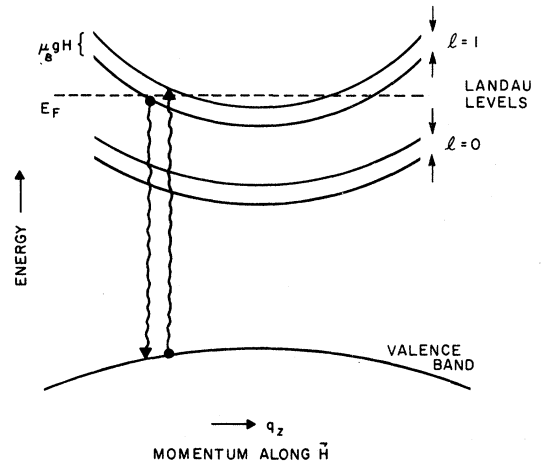

FIG. 1. Spin-flip scattering in a degenerate semiconductor. The valence band has mixed spin symmetry $a|\uparrow\rangle+b|\downarrow\rangle$ due to spin-orbit coupling.

II. LINEWIDTHS

In our earlier paper[1] we showed that in an external magnetic field one observes spin-flip transitions in these mobile carriers in CdS and ZnSe at frequencies

$$\omega_s=\mu_B gH/\hbar \quad , \tag{3}$$

in good agreement with those calculated using earlier estimates of the electron g values.[11] However, the observed linewidths Γ did not correlate well with those which were calculated from $\Gamma=1/T_1$. T_1 is the spin-lattice relaxation time given by Yafet's formula[12]

$$\frac{\tau}{T_1}\approx(2-g)^2\left(\frac{m^*}{m}\right)\left(\frac{kT}{E_g}\right)^2 \quad , \tag{4}$$

where τ is the collision time and E_g is the band gap. In the present work we have found that line-

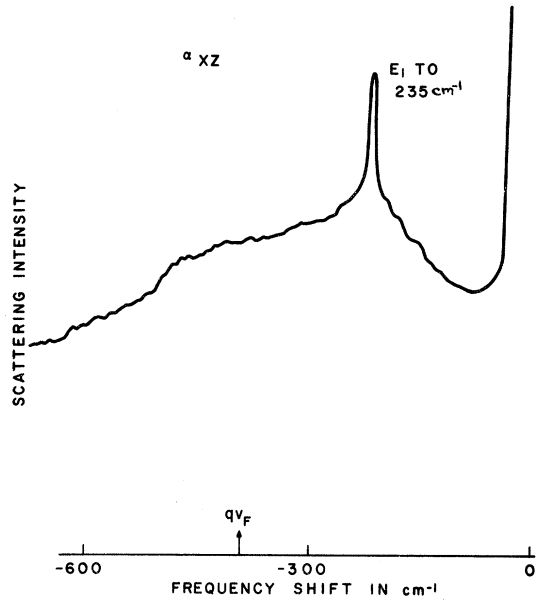

FIG. 2. Single-electron scattering in zero field at 10 °K for $n = 4\times10^{18}$ cm^{-3} CdS. α_{XZ} polarizability (Z = optic axis). The sharp line at 235 cm^{-1} is an E_1 symmetry TO phonon. $\lambda = 5145$ Å.

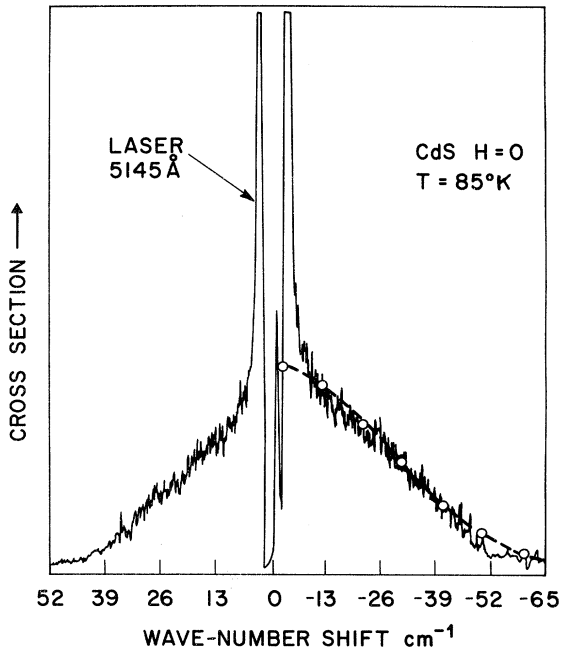

FIG. 3. Single-electron scattering in zero field at 85 °K for $n = 1\times10^{16}$ cm^{-3} CdS. The dot-dashed curve is a fit to the Gaussian profile of Eq. (2).

widths vary by nearly two orders of magnitude as temperature is varied from 2 to 150 °K, and are not lifetime dominated.

The linewidths (half-width at half-height) of two samples of CdS and ZnSe, each having $n \sim 5\times10^{17}$ cm^{-3} (indium doped), are shown versus temperature in Fig. 4. These data are for right-angle scattering at 5145 Å with an applied field of approximately 56 kG. Several other magnetic field strengths were employed, with no discernible change in linewidth. With the exception of low-temperature (< 10 °K) data in Fig. 4 taken with a Fabry–Perot interferometer, all the data presented were obtained with a Spex 0.75-m double monochromator and 20-μm slit width. The linewidths were determined by deconvoluting the observed line shape from the spectral response function of the spectrometer. Specifically, the assumed line shape [Eq. (5)] was combined with the instrumental response function, and the parameters appearing in (5) determined by the best fit to the observed spectral shape. This was performed numerically and yielded the line shape, as well as width, as shown in Figs. 5(a) and 5(b). The deconvoluted spectral distribution function $S(\omega)$ was found to be simply related to the free-spin susceptibility:

$$S(\omega) = -\frac{\bar{n}(\omega)+1}{\pi}\,\mathrm{Im}\chi_\perp(\omega) = \frac{\bar{n}(\omega)+1}{\pi}\chi_0\frac{\omega\Gamma}{(\omega-\omega_s)^2+\Gamma^2}\quad, \tag{5}$$

where $\bar{n}(\omega) = (e^{\hbar\omega/kT}-1)^{-1}$; χ_0 is the $\omega = 0$ susceptibility; ω_s is the Zeeman splitting $\mu_B g H/\hbar$; and Γ is a phenomenological frequency-independent damping constant. The expression for $\mathrm{Im}\chi_\perp(\omega)$ in Eq. (5) differs by a factor ω/ω_s from that usually quoted for the Bloch equations (6)–(8), and corresponds to the "modified" Bloch equations[13] in which the assumption that $\gamma H T_2 \gg 1$ is not required and the magnetization is taken to relax toward $\vec{H}$

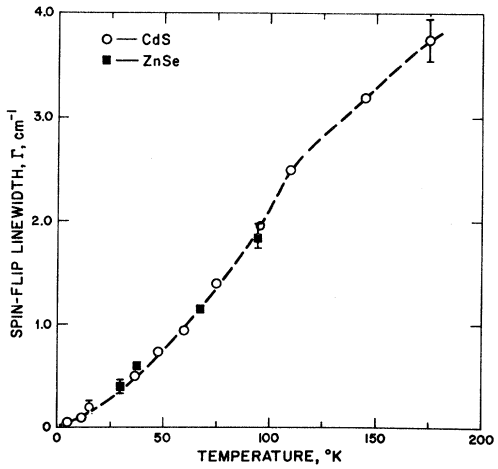

FIG. 4. Linewidth versus temperature in ZnSe and CdS having $n \sim 5\times10^{17}$ cm^{-3}. CdS data at 5145 Å; ZnSe at 4880 Å. 20-μm slit width; 56 kG. Right-angle scattering.

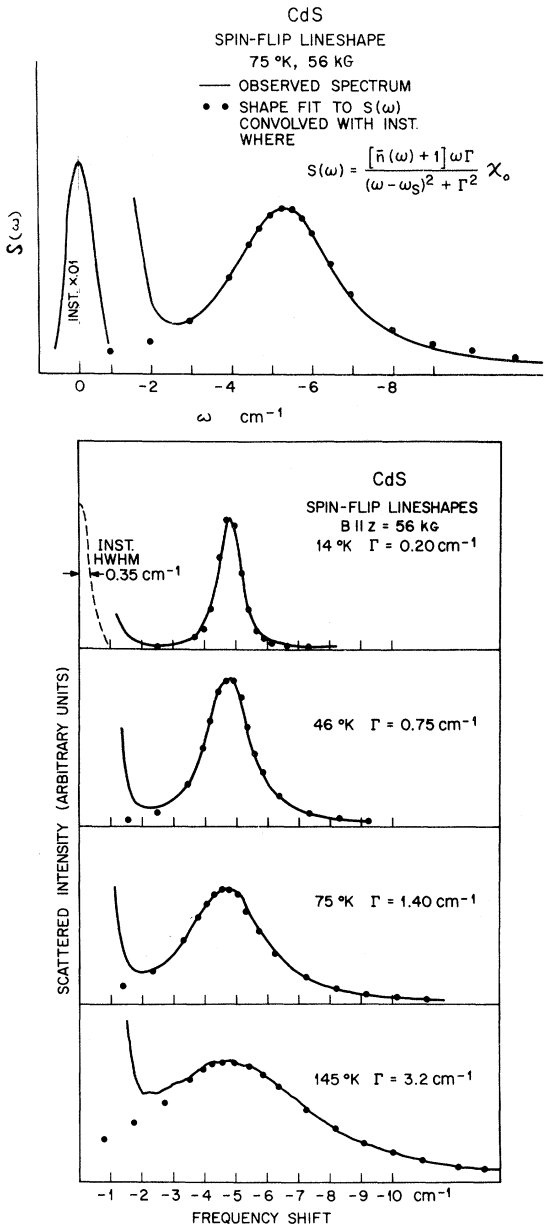

FIG. 5. (a) Line shape observed for right-angle scattering at 56 kG in $n = 5\times10^{17}$ cm^{-3} CdS at $T = 75$ °K. Dots are observed values; solid curve is calculated from Eq. (5). (b) Line shapes in CdS versus temperature, theory, and experiment, as in (a).

rather than toward $\vec{H}_0$:

$$\frac{dM_z}{dt} = \gamma(\vec{M}\times\vec{H})_z + \frac{\chi_0 H_z - M_z}{T_1}\ , \tag{6}$$

$$\frac{dM_x}{dt} = \gamma(\vec{M}\times\vec{H})_x + \frac{\chi_0 H_x - M_x}{T_2}\ , \tag{7}$$

$$\frac{dM_y}{dt} = \gamma(\vec{M}\times\vec{H})_y + \frac{\chi_0 H_y - M_y}{T_2}\ , \tag{8}$$

where $\gamma = -g\mu_B\hbar$; $\vec{M}$ is the magnetization; and $\vec{H}$ is the total field $H_0\hat{z} + \vec{H}_t(t)$, with $\vec{H}_0$ the applied static magnetic field and $\vec{H}_t$ the oscillating field at the spin frequency ω_s.

In relating Eq. (5) to Eqs. (6)–(8) one identifies Γ with $1/T_2$. However, in general the measured width for spin transitions will *not* be $1/T_2$, but will be dependent upon both homogeneous- and inhomogenous-broadening mechanisms. Whereas two different transverse relaxation times T_2 and T_2^* are commonly employed in NMR literature to describe such contributions to linewidths, we do not find it useful to make detailed contact with this terminology here. We do emphasize that T_1 estimated from Eq. (4) is several orders of magnitude larger than our measured $1/\Gamma$; thus, we believe longitudinal relaxation plays a negligible role in broadening ZnSe and CdS spin-flip-scattering lines.

Our measurements of linewidth for near-forward-direction scattering show that Γ increases from 0.05 cm^{-1} at 4 °K to 0.5 cm^{-1} at 100 °K. Since there is very small momentum transfer in this geometry the width receives negligible contribution from spin diffusion. The residual q-independent width is, therefore, a measure of spin lifetime and allows us to estimate T_2 as $\sim 7\times10^{-10}$ sec at 4 °K and $\sim 7\times10^{-11}$ sec at 100 °K. This is to be compared with a collision time τ of about 3×10^{-13} sec in the same samples, and T_1 estimated from Eq. (4) as 10^{-6} sec.

Angular Dependence

In addition to the temperature dependence reported above, we have measured the spin-flip linewidth as a function of momentum transfer q, or scattering angle θ ($q = 2K_L \sin\frac{1}{2}\theta$; K_L is the laser wave vector). Scattering angles of 0 °, 28 °, 90 °, and 152 ° were employed. The results for one CdS sample are summarized in Fig. 6, and in Figs. 7(a) and 7(b) actual data are shown to illustrate the dramatic line narrowing observed for small-angle scattering. This q dependence shows clearly that the linewidths presented in Fig. 4 are not due to spin lifetimes, but to spin diffusion. Such phenomena have been studied recently in InSb both experimentally and theoretically by Brueck, Mooradian, and Au Yang.[14,15] The basic interpretation is that of motional narrowing.

Motional narrowing is well understood in NMR and the analysis found in Kittel's text and elsewhere stems basically from the early work of Bloembergen, Purcell, and Pound.[16] Because the electrons in a crystal are in rapid relative motion, and because the electrons interact with each other (dipole-dipole interactions among the spins), the local field H_t fluctuates rapidly in time. The simplest algebraic treatment is that of Kittel[17] who supposes that the local field is H_t for a short

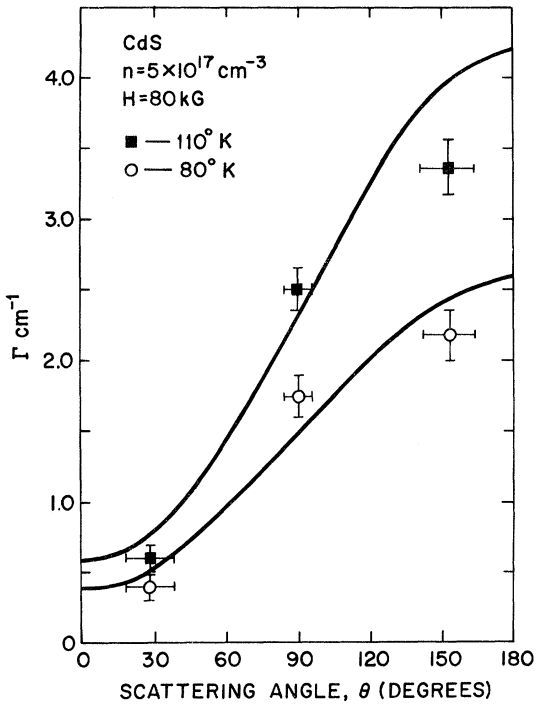

FIG. 6. Linewidth versus internal scattering angle for $n = 5 \times 10^{17}$ cm^{-3} CdS at $T = 80$ and 110 °K. Solid curves are of form $\Gamma(\theta, T) = A(T) + B(T)q^2$, where q is proportional to sin $(\frac{1}{2}\theta)$.

time τ and then changes by $\pm H_i$. During the time τ the spin will precess an extra $\pm \gamma H_i \tau$ compared to precession in the applied field H_0. After n time intervals of length τ the rms dephasing angle is

$$\langle \phi^2 \rangle^{1/2} = n^{1/2} \gamma H_i \tau \ , \tag{9}$$

assuming random-walk processes. Hence, the number of steps n necessary to dephase by 1 rad is, from (9),

$$n = 1 / \gamma^2 H_i^2 \tau^2 \ , \tag{10}$$

which occurs in time

$$T_2 = n\tau = 1 / \gamma^2 H_i^2 \tau \ . \tag{11}$$

Thus, the linewidth $\Gamma = 1 / T_2$ is given by

$$\Gamma = (\gamma H_i)^2 \tau = A\tau \ . \tag{12}$$

The ideas involved in motional narrowing and in spin diffusion are slightly different: In the first case, collisions prevent the spins from dephasing: in the second case, collisions prevent the spins from diffusing. In each case a linewidth proportional to τ is obtained.

Equations of the form given in (12) have been derived by both Brueck[14] and Au Yang[15] for spin-flip light scattering. Au Yang's formula for momentum transfer along H is

$$\Gamma_{\parallel} = 2q^2 (k_B T / m^*) \tau(T) \ , \tag{13}$$

where $\Gamma_{\parallel}$ is the linewidth for momentum transfer along the field direction; q is the momentum transfer $|\vec{K}_L - \vec{K}_S|$ with $K_L = 2\pi n \omega_L$, $K_S = 2\pi n \omega_S$, and ω_L, ω_S are the laser- and scattered-photon frequencies, respectively; $k_B T$, the thermal energy; m^*, the effective mass; and $\tau(T)$, the collision lifetime determined from Hall-mobility or plasmon-linewidth measurements. Wolff[18] has suggested that Eq. (13) can be modified for momentum transfer perpendicular to H by

$$\Gamma_{\perp} = \Gamma_{\parallel} / [1 + (\omega_c \tau)^2] \ , \tag{14}$$

where ω_c is the cyclotron-resonance frequency. In systems such as CdS or ZnSe, $\omega_c \tau < 1$ even at 100 kOe. Thus, $\Gamma_{\perp} \approx \Gamma_{\parallel}$. Physically, this means that spin diffusion transverse to $\vec{H}$ is about as likely as along $\vec{H}$ in low-mobility semiconductors.

As shown in Figs. 4 and 6, the two qualitative features of Eq. (13) have been experimentally confirmed for CdS in the present work, namely, the quadratic dependence upon q and linear (approximately) dependence upon T are verified. However, the absolute magnitude of Γ for large-angle scattering is about ten times less than calculated. The only parameter appearing in (13) which is sample dependent is the collision time τ. However, the data for Figs. 4–7 are for a sample having $\tau = 3 \times 10^{-13}$ sec as determined from Hall-mobility measurement. Thus we believe that the disagreement of a factor of 10 between theory and experiment for absolute linewidth represents a failure of the theory. McWhorter[19] has suggested that Eq. (13) may be generalized in a way to provide better accord with CdS data.

III. CROSS SECTIONS

Cross-section measurements have been made on a number of samples of CdS. These include commercially supplied material (Eagle Picher UHP, In, and Ga doped; samples from Harshaw; vapor-transport-grown platelets; and Br-doped platelets). No sample of CdS has been examined which did *not* exhibit either free- or bound-electron spin-flip scattering. In contrast, of the four ZnSe samples studied, only one showed spin-flip scattering. This sample from Eagle Picher was the most heavily doped of the four, containing a few times 10^{18} In per cm^3, according to spectrochemical analysis. (Compensation of the In results in a net estimated carrier concentration of the order 10^{17} cm^{-3}.

CdS and ZnSe samples having $n \sim 10^{17}$ cm^{-3} exhibited field-independent cross sections for 5145 Å excitation. From 40 to 95 kG the cross sections varied less than 10%. In contrast, one heavily doped CdS specimen ($n \sim 10^{19}$ cm^{-3}) exhibited a broad

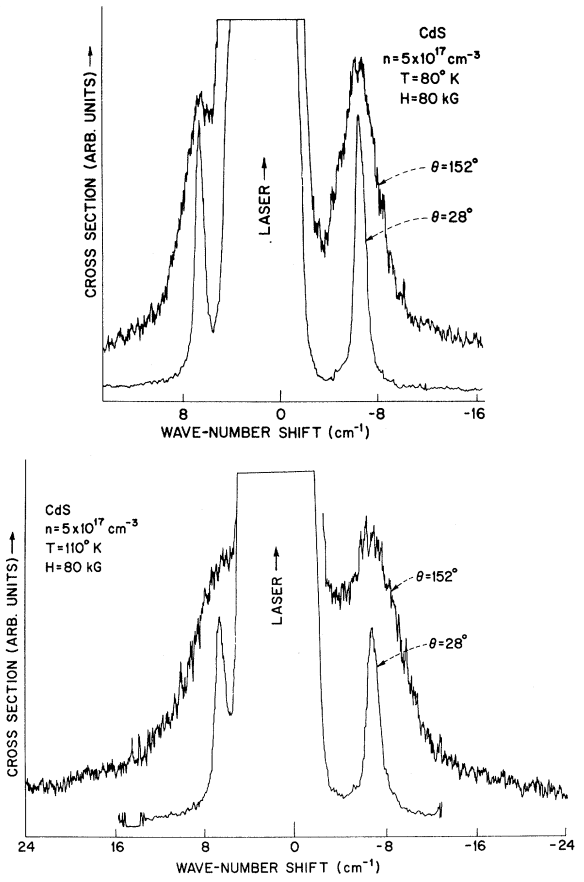

FIG. 7. (a) Line-shape data for 5×10^{17} cm^{-3} CdS at scattering angles $\theta=28°$ and 152°. $T=80$ °K. Slits 20 μ. (b) Line-shape data for 5×10^{17} cm^{-3} CdS at scattering angles $\theta=28°$ and 152°. $T=110$ °K. Slits 20 μ.

spin-flip-scattering spectrum whose integrated intensity varied roughly linearly in H (see Ref. 1).

Temperature dependences of cross sections in ZnSe and CdS were quite dramatically different. That for ZnSe at 5145-Å excitation is shown in Fig. 8; here the peak height is plotted. When this curve is multiplied by the linewidth (shown in Fig. 4), the resulting integrated intensity is found to decrease slowly with increasing T. However, in CdS ($n=5\times10^{17}$ cm^{-3}) the peak height is completely independent of T between 10 and 150 °K! Hence, the integrated intensity increased rapidly with increasing T, as implied by linewidth measurements in Fig. 4. We cannot explain these dependences in detail, but qualitative observations are in accord with this explanation: (i) As T increases the exciton states which act as intermediate states in the scattering process boraden out and become less effective (this is also observed in resonant-phonon scattering), thus decreasing the resonant cross section in ZnSe; (ii) in CdS this decrease is more than compensated by the fact that the band gap and exciton levels become more nearly resonant with the laser energy with increasing T.

The cross sections vary somewhat with scattering angle θ [see Figs. 7(a) and 7(b)]. However, this is difficult to measure quantitatively, due to the change in effective scattering volume and solid angle.

The change in cross section with angle Φ between $\vec{q}$ and $\vec{H}$ has already been noted.[1] Cross sections were eight times greater for $\vec{q}\cdot\vec{H}=0$ than for $\Phi=45°$. This has not been explained. The linewidth was also observed in Ref. 1 to increase by ~1 cm^{-1} for $\Phi=45°$. We can now attribute this to q_z transfer (z is the field direction), i.e., to nonvertical transitions in Fig. 1.

Finally, the cross sections measured are compatible with those given in Ref. 1 (~10^{-25} cm^2 per spin at 5145 Å) and about two orders of magnitude less than those given in Ref. 6 (for $\vec{q}\perp\vec{H}$ in both CdS and ZnSe).

The scattering was extremely resonant. CdS spin-flip scattering was observed at 5145, 5017, 4965, and 4880 Å and several intermediate frequencies, increasing by ~10^2 from 5145 to 4880 Å. It was also observed above the band gap at 4765 Å. The strong resonant cross sections together with the narrow linewidths observed in the forward

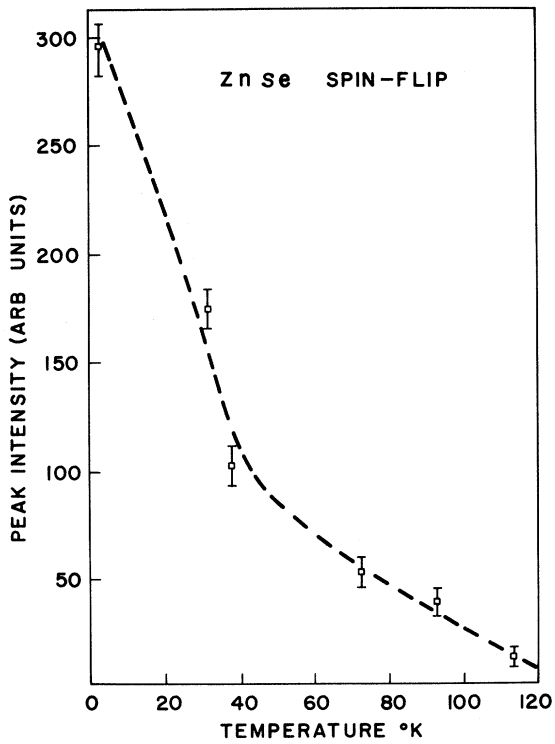

FIG. 8. Peak intensity for spin-flip scattering in ZnSe vs temperature. Right-angle scattering: $H=80$ kG.

direction have allowed us to produce *stimulated spin-flip* scattering in CdS. The spin-flip-scattering power output exhibited a sharp threshold at about 3 MW/cm^2 when pumped with 1 kW from an esculin dye laser at 4925 Å. Power output is shown versus input in Fig. 9. The dye laser was focused to 100-μm spot size and attenuated by means of calibrated neutral-density filters. A 1–10-Hz repetition rate was used with 500-nsec pulse length. Longitudinal pumping (forward scattering) with $\vec{q} \perp \vec{H}$ was employed. Other details will be published in a separate paper.

IV. SELECTION RULES

At moderate temperatures (80–300 °K) CdS and ZnSe with $n \sim 10^{17}$ cm^{-3} exhibit the expected free-spin selection rules: $\alpha_{ij} \neq 0$ only for $i \neq j$ and i or $j \| \vec{H}$. Despite the fact that CdS is uniaxial, no anisotropy of cross selections or g values is observed (i.e., $\vec{H} \| \vec{c}$ axis is the same as $\vec{H} \perp \vec{c}$; c = [0001]). These simple selection rules are not observed in some other systems; for example, they hold[15] in InSb at 5.3 μm but not[20] at 10.6 μm. We have found that these selection rules are also violated in CdS at low temperatures. As T decreases below 80 °K, both $\alpha_{xx} = \alpha_{yy}$ and $\alpha_{xz}(\vec{H} \| \vec{y})$ scattering become very strong. The scattering for these polarizability components is H independent, which is compatible with the selection rules of Ref. 6 for donor scattering from a C_{3v} symmetry site. It is not compatible with acceptor scattering. We interpret this observation as evidence that the free-electron scattering is dominated by more intense bound-electron scattering at low temperatures.

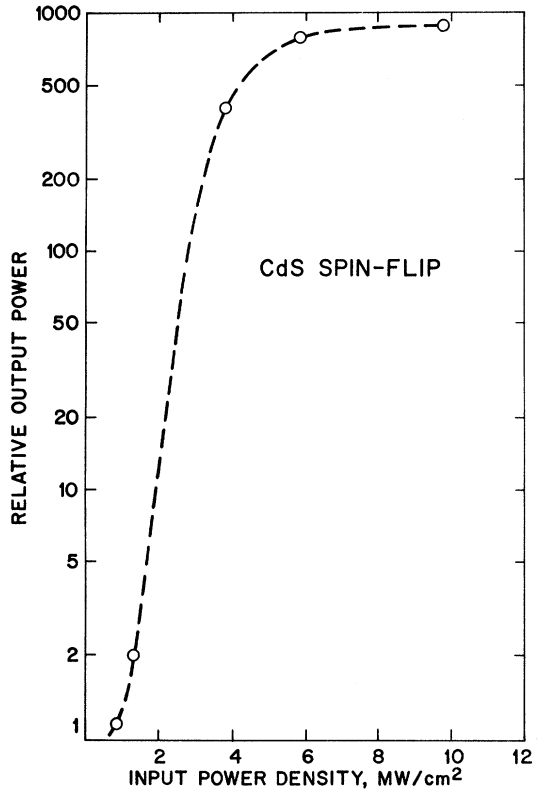

FIG. 9. Power output vs power input for spin-flip scattering in CdS, showing threshold at 3 MW/cm^2. Details are given in the text.

Additional evidence for bound-electron spin-flip scattering in low-carrier ($n \leq 5 \times 10^{17}$ cm^{-3}) CdS at low temperatures is manifest in the lack of thermalization for Stokes and anti-Stokes lines. For nominally pure CdS (Eagle Picher UHP), the Stokes–anti-Stokes ratio was nearly unity even at low temperatures (2.0 °K). Hence the electron population was "hot" and thermalization did not occur. In contrast, CdS and ZnSe having 10^{18}–10^{19} In or Ga showed complete thermalization (no detectable anti-Stokes intensity at 2 °K). This trend toward thermalization with increasing impurity concentration was also observed by Thomas and Hopfield[6] with Br-doped CdS. This has not been explained in detail, but it appears physically reasonable that thermalization should occur among spins when there are larger numbers of interacting spins.

V. DOUBLE SPIN-FLIP SCATTERING

Double spin-flip scattering has been observed in CdS samples having $n \leq 5 \times 10^{17}$ cm^{-3} with 4880-Å excitation. Typical data are shown in Fig. 10. In Fig. 11 the extremely narrow linewidth is shown clearly. For this $n \times 10^{16}$ cm^{-3} sample, the relative intensity of the double spin-flip to single spin-flip line is about 1.5%. This ratio is field independent at temperatures ≥ 10 °K, but decreases noticeably with increasing H at 2.0 °K, as shown in Fig. 12. Figure 12 also shows an inverse monotonic variation of $I(\Delta S = 2)/I(\Delta S = 1)$ with temperature.

The double spin-flip scattering is observed with equal intensity for α_{xx}, α_{xz}, and α_{xy} polarizability components ($\vec{z} \perp \vec{H}$), and is also observed only at low temperatures (≤ 25 °K). This is one indication that the double spin-flip process involves two donors and is not a free-electron process. We note that no $\Delta S = \pm 2$ processes have been previously observed via light scattering.[21]

The intensity ratio $I(\Delta S = 2)/I(\Delta S = 1)$ increases to about 10% in CdS samples doped to $\sim 10^{18}$ cm^{-3} with In or Ga donors at 90 kG and 2 °K. This further indicates that the double spin-flip process is a two-donor phenomenon. Spectra are shown for 10^{18} cm^{-3} In in Fig. 13.

It is significant that the $\Delta S = \pm 2$ energy shift is slightly less than twice that of $\Delta S = \pm 1$ (see

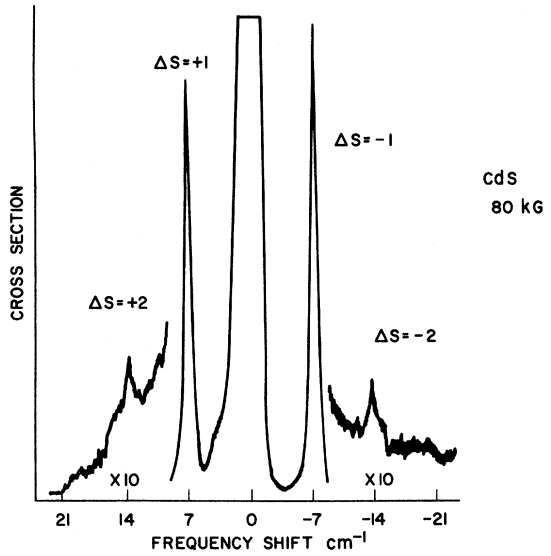

FIG. 10. Single and double spin-flip scattering in $n = 10^{16}$ cm^{-3} CdS. $H = 80$ kG. $T = 10$ °K. Note intensity scale changes.

Fig. 11). The discrepancy is between 0.03 and 0.04 meV (or 0.2–0.3 cm^{-1}) in our samples, and independent of field.

There are two possible interpretations of the small shift in $\omega(\Delta S = 2)$. The first is a ground-state spin interaction which results in dispersion.

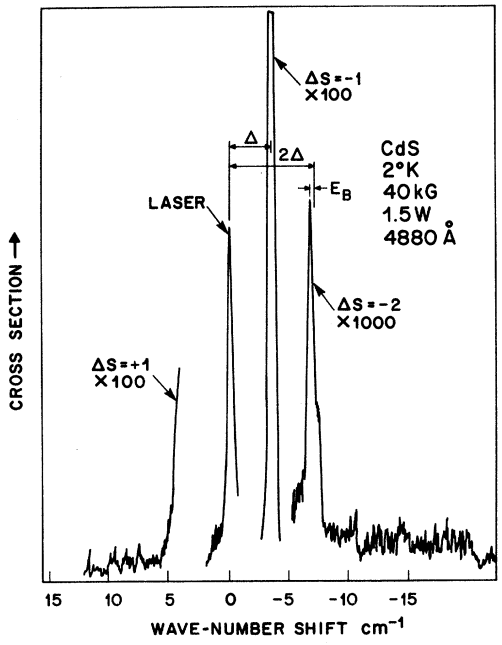

FIG. 11. Single and double spin-flip scattering in $n = 10^{16}$ cm^{-3} CdS. $H = 40$ kG. $T = 2.0$ °K. Note intensity scale changes.

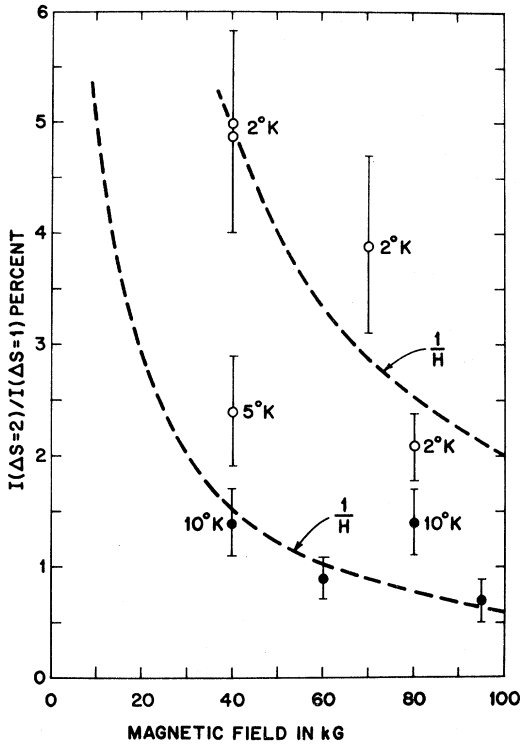

FIG. 12. Double-flip intensity divided by single-flip intensity vs field for several temperatures.

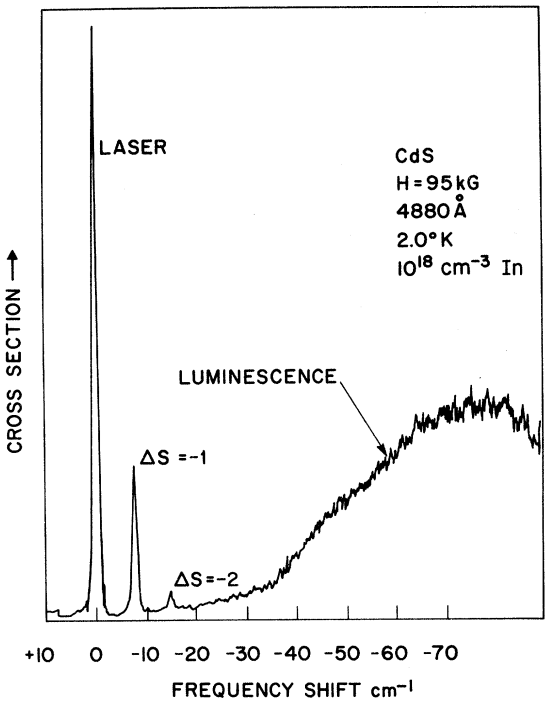

FIG. 13. Single and double spin-flip spectra in CdS with 10^{18} cm^{-3} In donors. Note the thermalization at 2.0 °K and 95 kG (no anti-Stokes lines).

Two single spin-flip transitions at $q = k$ and $q = -k$ could then give rise to a $\omega(\Delta S = 2)$ frequency less than twice $\omega(\Delta S = 1)$. A second mechanism is that of completely localized spins which do not interact in the ground state (electrons bound to donors), but which may interact by exchange in the excited state.[22] The 0.2–0.3-cm^{-1} shift of $\omega(\Delta S = 2)$ in this dispersionless case is viewed as an electron-pair binding energy. This model has been treated theoretically by Economou, Ruvalds, and Ngai,[23] who are able to account for the essential features of our $\Delta S = 2$ spectra. However, neither this theory nor the data presented here are sufficiently detailed to rule out wave-vector dispersion or slight spin-delocalization effects. It is important to note that any dispersion will modify the line shape, and that, therefore, a careful study of line shape and its dependence upon n, T, H, etc., will supply information on the degree of localization of the spins. Further experimental and theoretical work on this double spin-flip phenomenon is required.

Finally, we have observed a $\Delta S = -3$ process in one CdS sample (10^{18}-cm^{-3} In), which has 8–10% of the $\Delta S = -2$ line intensity and which lies at $[3\omega(\Delta S = 1) - 0.8\ \text{cm}^{-1}]$. Such higher-order processes are predicted in Ref. 23.

ACKNOWLEDGMENTS

Discussions with J. P. Gordon, J. Ruvalds, and Y. Yafet are gratefully acknowledged. The theoretical advice and suggestions of P. A. Wolff regarding linewidths have been invaluable. P. Lazay is to be thanked for assistance with the Fabry–Perot measurements and B. Tell for Hall measurements. A. DiGiovanni is to be credited for his careful maintenance and repair of the superconducting magnet.

---

*Present address: Department of Physics and Astrophysics, University of Colorado, Boulder, Colo.

[1]P. A. Fleury and J. F. Scott, Phys. Rev. B 3, 1979 (1971).

[2]Preliminary accounts of some of the results in the present paper were presented at several meetings in 1972: J. F. Scott, P. A. Fleury, and T. C. Damen, Bull. Am. Phys. Soc. 17, 335 (1972); J. F. Scott and T. C. Damen, J. Opt. Soc. Am. 62, 730A (1972); J. F. Scott, P. A. Fleury, and T. C. Damen, J. Quantum Electron. QE8, 531 (1972); and in Proceedings of the International Conference on Low-Temperature Physics (LT-13) (unpublished).

[3]R. E. Slusher, C. K. N. Patel, and P. A. Fleury, Phys. Rev. Letters 18, 77 (1967).

[4]C. K. N. Patel and R. E. Slusher, Phys. Rev. 167, 413 (1968).

[5]C. K. N. Patel and R. E. Slusher, Bull. Am. Phys. Soc. 13, 480 (1968); Phys. Rev. 177, 1200 (1969).

[6]D. G. Thomas and J. J. Hopfield, Phys. Rev. 175, 1021 (1968).

[7]For a discussion of spin-photon interaction mechanisms and of both first- and second-order spin-wave scattering in insulators, see P. A. Fleury and R. Loudon, Phys. Rev. 266, 514 (1968).

[8]J. F. Scott, R. C. C. Leite, T. C. Damen, and Jagdeep Shah, Phys. Rev. B 1, 4330 (1970).

[9]P. A. Wolff, in *Light Scattering Spectra of Solids*, edited by G. B. Wright (Springer-Verlag, New York, 1969), p. 273.

[10]D. C. Hamilton and A. L. McWhorter, Ref. 9, p. 309; A. Mooradian, Phys. Rev. Letters 20, 1102 (1968).

[11]M. V. Kurik, Fiz. Tekhn. Poluprov. 3, 1260 (1969) [Sov. Phys. Semicond. 3, 1056 (1970)]. [We found g(ZnSe) $= 1.18 \pm 0.03$ and g(CdS) $= 1.86 \pm 0.04$.]

[12]Y. Yafet, Solid State Phys. 14, 1 (1963).

[13]A. Abragam, *Principles of Nuclear Magnetism* (Clarendon, Oxford, 1961), pp. 53 and 54. Because our linewidths are diffusion dominated at high temperatures and large scattering angles, as shown by the q dependence in Figs. 6–8, the line-shape derivation in Eqs. (5)–(8) is justified for only the low-temperature or small-angle data. However, the Lorentzian form of Eq. (5) is also obtained theoretically for inhomogeneous broadening mechanisms, so the fitting procedure used is in fact valid for the general case. See Refs. 14 and 15.

[14]S. R. J. Brueck, Ph.D. thesis (MIT, 1971) (unpublished); S. R. J. Brueck and A. Mooradian, Phys. Rev. Letters 28, 161 (1972).

[15]Y. C. S. Au Yang, Ph.D. thesis (MIT, 1971) (unpublished).

[16]N. Bloembergen, E. M. Purcell, and R. V. Pound, Phys. Rev. 73, 679 (1948).

[17]Charles Kittel, *Introduction to Solid State Physics* (Wiley, New York, 1968), 3rd ed., pp. 518 and 519.

[18]P. A. Wolf (private communication).

[19]A. L. McWhorter (private communication).

[20]C. K. N. Patel and K. H. Yang, Appl. Phys. Letters 18, 491 (1971).

[21]The two-magnon data of Ref. 7 in antiferromagnets involve pairs of spin excitations whose total $\Delta S = 0$. Whereas $\Delta S = 2$ magnon transitions have been treated theoretically, none have been observed.

[22]There exists ample evidence for both ground- and excited-state exchange effects among localized spins in magnetic insulators. See, for example, R. J. Elliott, M. F. Thorpe, G. Imbusch, R. Loudon, and J. B. Parkinson, Phys. Rev. Letters 21, 147 (1968); P. A. Fleury, *ibid.* 21, 151 (1968).

[23]E. N. Economou, J. Ruvalds, and K. L. Ngai, Phys. Rev. Letters 29, 109 (1972); J. F. Scott and T. C. Damen, *ibid.* Letters 29, 107 (1972).